Performance Analysis of QAM Systems Under Class A Impulsive Noise Environment

Shinichi Miyamoto, *Member, IEEE*, Masaaki Katayama, *Member, IEEE*, and Norihiko Morinaga, *Senior Member, IEEE*

Abstract— **This paper describes the performance of QAM (Quadrature Amplitude Modulation) systems under impulsive noise environment. In the analysis, we employ, as a model of the impulsive noise, Middleton's model labeled class A. First, the statistical characteristics of the in-phase and quadrature components of the impulsive noise are investigated, and it is proved that, in contrast to Gaussian noise, these components are dependent especially for the impulsive noise with small impulsive indices. Next, with consideration of the dependence between the in-phase and quadrature components of the noise, the performance of QAM systems with the conventional receiver designed for Gaussian noise is analyzed. The numerical results show that the performance is much worse than that achieved under Gaussian noise. Moreover, we show the design of the maximum likelihood receiver for class A impulsive noise and the great performance improvement by this receiver is confirmed.**

I. Introduction

QAM (Quadrature Amplitude Modulation) is a modulation scheme which provides high frequency spectrum efficiency. For the terrestrial radio communication systems with fixed stations, this modulation scheme has long been used [1], and recently the use of QAM even in mobile radio communication systems is receiving attention [2].

In most of previous performance analysis of QAM systems, the noise presented at the receiver's front end has been assumed to be Gaussian. In recent years, however, a variety of man-made noise (e.g., ignition noise, powerline noise), which are the major causes of errors in digital radio communication systems, are impulsive and their statistical characteristics are much different from those of Gaussian noise. Therefore, the performances of QAM systems under impulsive noise environment have to be investigated.

As a statistical-physical model of the impulsive radio noise, the model named class A has been proposed [3], and the performances of ASK (Amplitude Shift Keying), FSK (Frequency Shift Keying), and PSK (Phase Shift Keying) systems with this class of noise have been investigated [4], [5]. As for the QAM systems, however, only the performance of the conventional receiver, which is designed for Gaussian noise, has been studied under the assumption that the in-phase and quadrature components of the impulsive noise are independent [6].

In this paper, we investigate the statistical characteristics of the in-phase and quadrature components of the class A impulsive noise, and with the consideration of its statistical characteristics, we analyze the performance of QAM systems under class A impulsive noise environment. In Section II, we discuss the statistical characteristics of the in-phase and quadrature components of the class A impulsive noise, and show that these components are not independent. In the succeeding section, we derive the symbol error probability of QAM systems with the conventional receiver designed for Gaussian noise. For comparison, we also show the results obtained with a coarse assumption ignoring the dependence between the in-phase and quadrature components of the impulsive noise. In Section IV, we give the configuration of the optimum receiver designed for class A impulsive noise [7], [8], and investigate the performance improvement achieved with this receiver.

II. Class A Impulsive Noise Model

A. Probability Density Functions of In-Phase and Quadrature Components

Middleton's canonical impulsive noise model is often used as a statistical-physical model of the impulsive radio noise. In this model, according to the relation between the durations of noise impulses and the spectral bandwidth at the receiver's ARI (Aperture-RF-IF), the impulsive noise is classified into three general classes, i.e., class A, B, and C [3]. In this paper, we focus on the class A noise model, in which the transients at the receiver's ARI can be ignored.

Though some experimental measurements of the actual impulsive noise supports the Middleton's canonical class A model, it is also reported that this model does not stand for some physical situations [9], and thus the quasi-canonical model with an additional correction series to a canonical formula has been proposed [10]. We, however, expect that the additional correction series affect little the physical meanings of the results obtained in this paper. Consequently, in order to simplify the analysis, we employ the original canonical class A model.

In general, a narrowband noise $n(t)$ is represented by its envelope $\xi(t)$ and phase $\phi(t)$ as

$$n(t) = \xi(t)\cos(2\pi f_c t + \phi(t)), \tag{1}$$

Manuscript received May 3, 1993; revised December 13, 1994.

S. Miyamoto and N. Morinaga are with the Department of Communication Engineering, Faculty of Engineering, Osaka University, Yamada-oka 2-1, Suita, Osaka 565, Japan.

M. Katayama is with the Department of Information Electronics, School of Engineering, Nagoya University, Furo-cho, Chikusa, Nagoya 464-01, Japan.

IEEE Log Number 9410268.

where f_c is a center frequency of the noise. Now let $n(t)$ be the class A impulsive noise whose power is normalized to be unity, i.e., $\overline{n^2(t)} = 1$. Then, according to [11], the probability density functions (pdf's) of the noise envelope $\xi(t)$ and phase $\phi(t)$ are given as

$$p_\xi(\xi) = e^{-A} \sum_{m=0}^{\infty} \frac{A^m 2\xi}{m! 2\sigma_m^2} \exp\left(-\frac{\xi^2}{2\sigma_m^2}\right) \tag{2}$$

and

$$p_\phi(\phi) = \frac{1}{2\pi} \qquad (0 \le \phi < 2\pi), \tag{3}$$

where

$$\sigma_m^2 = \frac{m/A + \Gamma'}{1 + \Gamma'}. \tag{4}$$

In the above equations, Γ' is the mean power ratio of the Gaussian noise component to the non-Gaussian noise component, and A is the impulsive index, i.e., the product of the received average number of impulses per unit time and the duration of an impulse. The impulsive index A defines the "impulsiveness" of the noise. For the smaller impulsive index A, the noise becomes more impulsive, and on the contrary, for the larger impulsive index A, the statistical characteristics of class A impulsive noise approach those of Gaussian noise (for example, in case of $A = 10$, the class A impulsive noise can be regarded as Gaussian noise).

The noise $n(t)$ can be also represented by its in-phase component $x(t)$ and quadrature component $y(t)$ as

$$n(t) = x(t) \cos 2\pi f_c t - y(t) \sin 2\pi f_c t, \tag{5}$$

where

$$x(t) = \xi(t) \cos \phi(t), \quad y(t) = \xi(t) \sin \phi(t) \tag{6}$$

and

$$\xi(t) = \sqrt{x^2(t) + y^2(t)}, \tag{7}$$

$$\phi(t) = \tan^{-1} \frac{y(t)}{x(t)}. \tag{8}$$

Now let us derive the joint pdf of these components and the pdf's of each component. From (5)–(8), the joint pdf of the in-phase and quadrature components $p_{x,y}(x, y)$ is represented as

$$\begin{aligned} p_{x,y}(x, y) &= \frac{\partial(x, y)}{\partial(\xi, \phi)} p_{\xi,\phi}(\xi, \phi) \\ &= \frac{1}{(x^2 + y^2)^{1/2}} p_{\xi,\phi}(\xi, \phi). \end{aligned} \tag{9}$$

Since the noise envelope $\xi(t)$ and phase $\phi(t)$ are statistically independent, (9) becomes

$$\begin{aligned} p_{x,y}(x, y) &= \frac{1}{(x^2 + y^2)^{1/2}} p_\phi(\phi) p_\xi(\xi) \\ &= \frac{1}{2\pi (x^2 + y^2)^{1/2}} p_\xi(\xi). \end{aligned} \tag{10}$$

Substituting the pdf of the noise envelope (2) into (10), we obtain the joint pdf of the in-phase and quadrature components as

$$p_{x,y}(x, y) = e^{-A} \sum_{m=0}^{\infty} \frac{A^m}{m! 2\pi\sigma_m^2} \exp\left(-\frac{x^2 + y^2}{2\sigma_m^2}\right). \tag{11}$$

Integrating (11) with respect to x and y, therefore, we can also obtain the pdf's of each component as

$$p_x(x) = e^{-A} \sum_{m=0}^{\infty} \frac{A^m}{m! \sqrt{2\pi\sigma_m^2}} \exp\left(-\frac{x^2}{2\sigma_m^2}\right), \tag{12}$$

$$p_y(y) = e^{-A} \sum_{m=0}^{\infty} \frac{A^m}{m! \sqrt{2\pi\sigma_m^2}} \exp\left(-\frac{y^2}{2\sigma_m^2}\right). \tag{13}$$

B. Correlation and Dependence between In-phase and Quadrature Components

The cross correlation between the in-phase component x and the quadrature component y is obtained as

$$\begin{aligned} \overline{xy} &= \int_{-\infty}^{\infty} \int_{-\infty}^{\infty} xy p(x, y)\, dx\, dy \\ &= \sum_{m=0}^{\infty} \frac{A^m}{m! 2\pi\sigma_m^2} \int_{-\infty}^{\infty} x e^{-(x^2/2\sigma_m^2)}\, dx \\ &\quad \cdot \int_{-\infty}^{\infty} y e^{-(y^2/2\sigma_m^2)}\, dy \\ &= 0. \end{aligned} \tag{14}$$

Hence, the in-phase and quadrature components of the class A impulsive noise are uncorrelated. On the other hand, from (11)–(13), it is clear that the joint pdf of the in-phase and quadrature components $p_{x,y}(x, y)$ is not equal to the product of the pdf's of each component $p_x(x)p_y(y)$, i.e., the in-phase and quadrature components of class A impulsive noise are not statistically independent. Therefore, we can see that a pair of the in-phase and quadrature components of the class A impulsive noise is a good example of stochastic processes which are uncorrelated but dependent.

Let us now investigate the dependence between the in-phase and quadrature components of class A impulsive noise more in detail. The joint pdf of the in-phase and quadrature components $p_{x,y}(x, y)$ and the product of the pdf's of each component $p_x(x)p_y(y)$ are shown in Fig. 1 for the impulsive index $A = 10$ and in Fig. 2 for $A = 0.1$.

In Fig. 1, the shape of $p_x(x)p_y(y)$ is almost same as that of $p_{x,y}(x, y)$. Hence, for $A = 10$, the in-phase and quadrature components of the class A impulsive noise can approximately be considered to be independent. This seems to be a reasonable result, because the class A impulsive noise behaves as Gaussian noise with a large impulsive index such as $A = 10$. On the other hand, in Fig. 2, in the case of $A = 0.1$, $p_{x,y}(x, y)$ and $p_x(x)p_y(y)$ have quite different shapes. Consequently, for the smaller impulsive index (the more impulsive noise), the assumption that the in-phase and quadrature components of the impulsive noise are independent is no more applicable, that is, they are dependent processes. In fact, if they were statistically independent, then, as in Fig. 2(a),

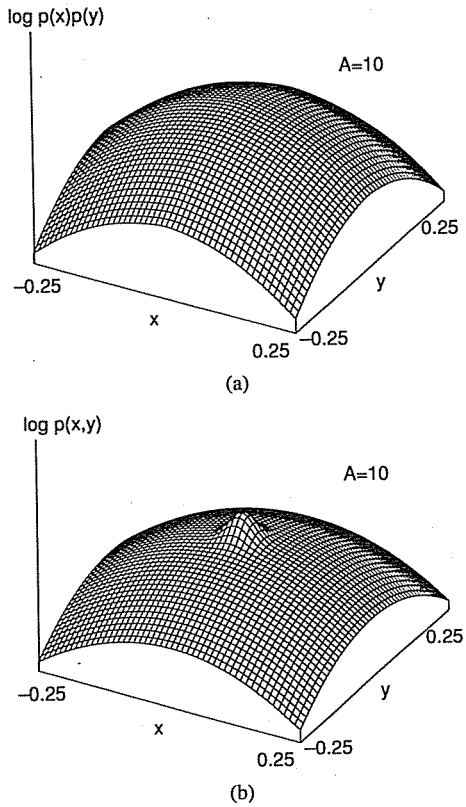

Fig. 1. (a) Product of the pdf's of the in-phase and quadrature components of the impulsive noise $p_x(x)p_y(y)$ (Impulsive index $A = 10$). (b) Joint pdf of the in-phase and quadrature components of the impulsive noise $p_{x,y}(x, y)$ (Impulsive index $A = 10$).

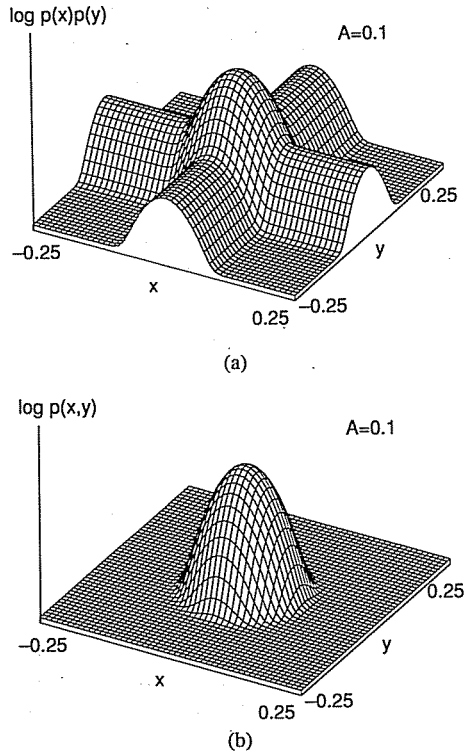

Fig. 2. (a) Product of the pdf's of the in-phase and quadrature components of the impulsive noise $p_x(x)p_y(y)$ (Impulsive index $A = 0.1$). (b) Joint pdf of the in-phase and quadrature components of the impulsive noise $p_{x,y}(x, y)$ (Impulsive index $A = 0.1$).

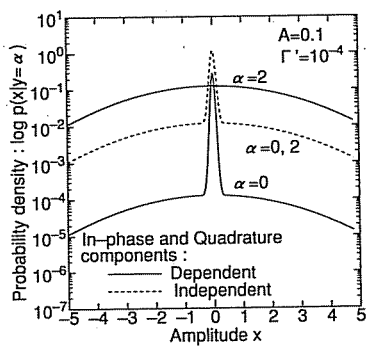

Fig. 3. Conditional pdf $p(x|y = \alpha)$ of the class A impulsive noise ($\alpha = 0.2$).

the pdf of the phase of the noise should be nonuniform distribution, which contradicts the basic definition (3).

On the dependence of the in-phase and quadrature components of the impulsive noise, let us discuss from another viewpoint. The conditional pdf

$$p(x|y = \alpha) = \frac{p_{x,y}(x, \alpha)}{p_y(\alpha)} \tag{15}$$

is given by solid lines in Fig. 3. If the in-phase and quadrature components of the noise were independent, this conditional pdf could be assumed to be $p_x(x)$, as shown by dashed lines. Comparing these two sets of lines, we understand as follows. If the in-phase and quadrature components could be assumed to be independent, the conditional pdf's should have the same distribution for any α as shown by dashed line. This is, however, not the actual phenomenon. Under the actual impulsive noise environment, as shown by solid lines, the probability that high amplitude noise is emitted in the in-phase component becomes larger for the larger α. In other words, if the impulse noise is emitted in the quadrature component, the probability that the impulse noise is emitted in the in-phase component becomes large.

III. Performance Analysis of M-ary QAM System with a Conventional Receiver

In this section, we analyze the performance of the M-ary QAM systems with the conventional receiver under class A impulsive noise environment. We first derive the symbol error probability of M-ary QAM systems ignoring the dependence of the in-phase and quadrature components of the impulsive noise as done in [6], and then we give the performance with the proper consideration of the dependence.

The M-ary QAM signal, whose signal constellation is shown in Fig. 4, is represented as

$$s(t) = \sum_{l=-\infty}^{\infty} \{a_l g(t - lT_S) \cos 2\pi f_c(t - lT_S) + b_l g(t - lT_S) \sin 2\pi f_c(t - lT_S)\}, \tag{16}$$

where f_c and T_S are the carrier frequency and the symbol duration of QAM signal, respectively , and the signal amplitudes a_l, b_l are

$$a_l, b_l \in \{\pm 1, \pm 3, \cdots, \pm\sqrt{M} - 1\}. \tag{17}$$

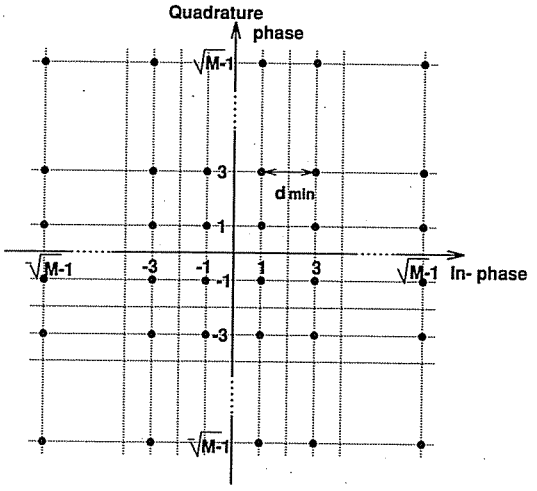

Fig. 4. Signal constellation for M-ary QAM signal.

In (16), $g(t)$ is the impulse response of the filter which generates the transmitted pulse given by

$$g(t) = 1 \qquad (0 \le t \le T_S). \tag{18}$$

Let $d_{\min}$ be the minimum distance between the signal points shown in Fig. 4. Then the average carrier power of M-ary QAM signal S_{av} is given as

$$S_{av} = \frac{d_{\min}^2}{12}(M-1). \tag{19}$$

Note that S_{av} is equal to the average Carrier to Noise power Ratio (CNR), since the noise is normalized to have unit power.

To obtain the symbol error probability of M-ary QAM systems with the conventional receiver, we classify the errors into three patterns as shown in Fig. 5, since the pdf of the noise phase is uniform distribution, where Fig. 5(a)–(c) show the error patterns for the transmitted signal points on the corners, on the sides, and on the other points of the signal constellation, respectively. The priori probabilities of three patterns are given as

$$P(a) = \frac{4}{M}, \quad P(b) = \frac{4(\sqrt{M}-2)}{M}, \quad P(c) = \frac{M-4(\sqrt{M}-1)}{M} \tag{20}$$

under the condition that the signal points are equally probable. Let P_{ea}, P_{eb}, and P_{ec} be the symbol error probabilities, which correspond to Fig. 5(a)–(c), then the symbol error probability of M-ary QAM systems Pe is given as

$$Pe = P(a)P_{ea} + P(b)P_{eb} + P(c)P_{ec}. \tag{21}$$

A. Symbol Error Probability with the Assumption of Independent In-phase and Quadrature Components

In this subsection, we derive the symbol error probability of QAM systems ignoring the dependence between the in-phase and quadrature components of the impulsive noise. Using (12) and (13), the symbol error probabilities P_{ea}, P_{eb}, and P_{ec} are

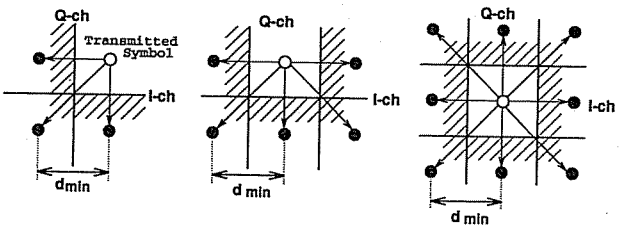

Fig. 5. Symbol error patterns of QAM signals.

derived as

$$\begin{aligned}
P_{ea} &= 1 - \int_{-d_{\min}/2}^{\infty} p_x(x)\,dx \int_{-d_{\min}/2}^{\infty} p_y(y)\,dy \\
&= 1 - \left\{ e^{-A} \sum_{m=0}^{\infty} \frac{A^m}{m!2} \operatorname{erfc}\left(-\frac{d_{\min}}{2\sqrt{2}\sigma_m} \right) \right\}^2, \\
P_{eb} &= 1 - \int_{-d_{\min}/2}^{d_{\min}/2} p_x(x)\,dx \int_{-d_{\min}/2}^{\infty} p_y(y)\,dy \\
&= 1 - \left\{ e^{-A} \sum_{m=0}^{\infty} \frac{A^m}{m!} \left(1 - \operatorname{erfc}\left(\frac{d_{\min}}{2\sqrt{2}\sigma_m} \right) \right) \right\} \\
&\quad \cdot \left\{ e^{-A} \sum_{m=0}^{\infty} \frac{A^m}{m!2} \operatorname{erfc}\left(-\frac{d_{\min}}{2\sqrt{2}\sigma_m} \right) \right\}, \\
P_{ec} &= 1 - \int_{-d_{\min}/2}^{d_{\min}/2} p_x(x)\,dx \int_{-d_{\min}/2}^{d_{\min}/2} p_y(y)\,dy \\
&= 1 - \left\{ e^{-A} \sum_{m=0}^{\infty} \frac{A^m}{m!} \left(1 - \operatorname{erfc}\left(\frac{d_{\min}}{2\sqrt{2}\sigma_m} \right) \right) \right\}^2.
\end{aligned} \tag{22}$$

As the results, the symbol error probability of QAM systems with the conventional receiver is obtained as

$$\begin{aligned}
Pe = \frac{4}{M} &\left[1 - \left\{ e^{-A} \sum_{m=0}^{\infty} \frac{A^m}{m!2} \right. \right. \\
&\left. \left. \cdot \operatorname{erfc}\left(-\frac{\sqrt{3}\sqrt{S_{av}}}{\sqrt{2}\sqrt{M-1}\sigma_m} \right) \right\}^2 \right] \\
&+ \frac{4(\sqrt{M}-2)}{M} \left[1 - \left\{ e^{-A} \sum_{m=0}^{\infty} \frac{A^m}{m!} \right. \right. \\
&\left. \cdot \left(1 - \operatorname{erfc}\left(\frac{\sqrt{3}\sqrt{S_{av}}}{\sqrt{2}\sqrt{M-1}\sigma_m} \right) \right) \right\} \cdot \\
&\left. \cdot \left\{ e^{-A} \sum_{m=0}^{\infty} \frac{A^m}{m!2} \operatorname{erfc}\left(-\frac{\sqrt{3}\sqrt{S_{av}}}{\sqrt{2}\sqrt{M-1}\sigma_m} \right) \right\} \right] \\
&+ \frac{M-4(\sqrt{M}-1)}{M} \left[1 - \left\{ e^{-A} \sum_{m=0}^{\infty} \frac{A^m}{m!} \right. \right. \\
&\left. \left. \cdot \left(1 - \operatorname{erfc}\left(-\frac{\sqrt{3}\sqrt{S_{av}}}{\sqrt{2}\sqrt{M-1}\sigma_m} \right) \right) \right\}^2 \right].
\end{aligned} \tag{23}$$

Note that this is a coarse approximation.

B. Symbol Error Probability with Consideration of the Dependence between the In-phase and Quadrature Components

In this subsection, considering the dependence between the in-phase and quadrature components of the impulsive noise, we derive the symbol error probability of QAM systems. Using the joint pdf of the both components (11), we obtain the error probabilities P_{ea}, P_{eb}, and P_{ec} as

$$\begin{aligned}
P_{ea} &= 1 - \int_{-d_{\min}/2}^{\infty}\int_{-d_{\min}/2}^{\infty} p_{x,y}(x,y)\,dx\,dy \\
&= 1 - e^{-A}\sum_{m=0}^{\infty}\frac{A^m}{m!4}\left\{\operatorname{erfc}\left(-\frac{d_{\min}}{2\sqrt{2}\sigma_m}\right)\right\}^2, \\
P_{eb} &= 1 - \int_{-d_{\min}/2}^{\infty}\int_{-d_{\min}/2}^{d_{\min}/2} p_{x,y}(x,y)\,dx\,dy \\
&= 1 - e^{-A}\sum_{m=0}^{\infty}\frac{A^m}{m!2}\left\{\left(1-\operatorname{erfc}\left(\frac{d_{\min}}{2\sqrt{2}\sigma_m}\right)\right)\right. \\
&\quad \left.\cdot\left(\operatorname{erfc}\left(-\frac{d_{\min}}{2\sqrt{2}\sigma_m}\right)\right)\right\}, \\
P_{ec} &= 1 - \int_{-d_{\min}/2}^{d_{\min}/2}\int_{-d_{\min}/2}^{d_{\min}/2} p_{x,y}(x,y)\,dx\,dy \\
&= 1 - e^{-A}\sum_{m=0}^{\infty}\frac{A^m}{m!}\left\{1-\operatorname{erfc}\left(\frac{d_{\min}}{2\sqrt{2}\sigma_m}\right)\right\}^2. \qquad (24)
\end{aligned}$$

From (19)–(21), and (24), the symbol error probability with the proper consideration of the dependence between the in-phase and quadrature components of the noise becomes

$$\begin{aligned}
Pe &= P(a)P_{ea} + P(b)P_{eb} + P(c)P_{ec} \\
&= \frac{4}{M}\left[1 - e^{-A}\sum_{m=0}^{\infty}\frac{A^m}{m!4}\right. \\
&\quad \left.\cdot\left\{\operatorname{erfc}\left(-\frac{\sqrt{3}\sqrt{S_{av}}}{\sqrt{2}\sqrt{M-1}\sigma_m}\right)\right\}^2\right] + \frac{4(\sqrt{M}-2)}{M} \\
&\quad \cdot\left[1 - e^{-A}\sum_{m=0}^{\infty}\frac{A^m}{m!2}\left\{1-\operatorname{erfc}\left(\frac{\sqrt{3}\sqrt{S_{av}}}{\sqrt{2}\sqrt{M-1}\sigma_m}\right)\right\}\right. \\
&\quad \left.\cdot\left\{\operatorname{erfc}\left(-\frac{\sqrt{3}\sqrt{S_{av}}}{\sqrt{2}\sqrt{M-1}\sigma_m}\right)\right\}\right] \\
&\quad + \frac{M-4(\sqrt{M}-1)}{M}\left[1 - e^{-A}\sum_{m=0}^{\infty}\frac{A^m}{m!}\right. \\
&\quad \left.\cdot\left\{1-\operatorname{erfc}\left(-\frac{\sqrt{3}\sqrt{S_{av}}}{\sqrt{2}\sqrt{M-1}\sigma_m}\right)\right\}^2\right]. \qquad (25)
\end{aligned}$$

C. Numerical Examples and Discussion

Fig. 6 shows the performance of 16QAM ($M = 16$) systems with the conventional receiver under class A impulsive noise environment. In this figure, dashed lines show the symbol error probabilities obtained by (23) under the assumption that the in-phase and quadrature components are independent, and solid lines show those obtained by (25) with the proper treatment of the dependence.

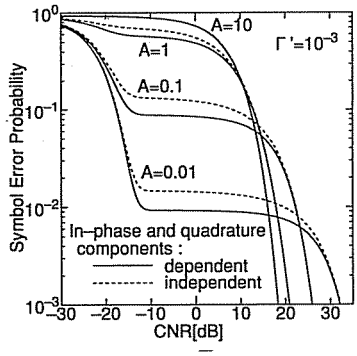

Fig. 6. Symbol error probabilities of QAM systems with the conventional receiver.

In Fig. 6, when $A = 10$, solid line and dashed line are almost the same. For the smaller impulsive indices ($A \leq 1$), on the other hand, these performances are quite different. This result comes from that given in Section II. Namely, for the large impulsive index A =10, the in-phase and quadrature components may be considered to be independent, however, for the smaller impulsive indices (i.e., the more impulsive noise), the assumption that the in-phase and quadrature components of the impulsive noise are independent is no more applicable. Also in this figure, for the small impulsive indices, the performance ignoring the dependence between the in-phase and quadrature components of the noise is worse than that obtained with the proper consideration of the dependence between these components. Especially, at relatively low CNR (-15 dB $\leq$ CNR $\leq$ 10 dB), in which the error probability depends on the number of symbols corrupted by impulse noise, the difference between these performances is quite large. This result is explained as follows.

Fig. 7(a) and (b) show the waveform models of the impulsive noise for the case that the in-phase and quadrature components of the noise are assumed to be independent and the case that these components are dependent, respectively. Here, suppose that one impulse noise (high amplitude noise) is emitted in each component during observation interval, therefore two impulse noises are observed in total. In independent case (Fig. 7(a)), the two impulse noises may be emitted in different two symbol durations because of their independency, and consequently two symbol decision errors may occur. On the other hand, under the actual impulsive noise environment (i.e., dependent case Fig. 7(b)), since the probability that the two impulse noises are emitted in the same symbol duration is high, the symbol decision error may occur in only one symbol duration. Therefore, the better symbol error performance can be obtained for the actual situation (or the dependent case).

In Fig. 6, at relatively high CNR ($\geq$ 20 dB), as the impulsive index A decreases, the performances of QAM systems with the conventional receiver are degraded largely. At symbol error probability $Pe = 10^{-3}$, for example, with the impulsive index $A = 10$, in which the statistical characteristics of class A impulsive noise are almost the same as those of Gaussian noise, the required CNR is about 18 dB. On the other hand,

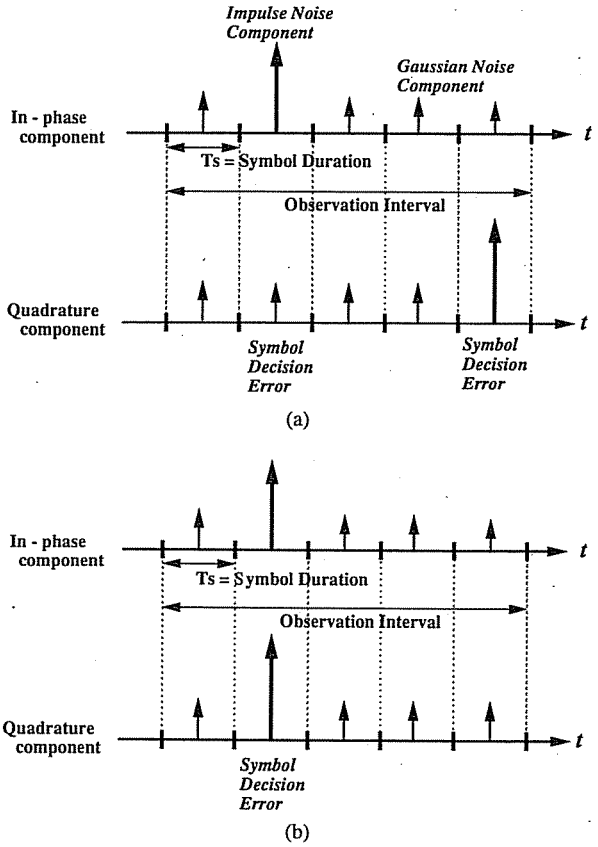

Fig. 7. Error mechanism due to impulsive noises. (a) Independent. (b) Dependent.

with $A = 0.1$, in which the noise is more impulsive, the required CNR is about 26 dB. This fact implies the necessity of the receiver robust against impulsive noise, which is discussed in the following section.

IV. Performance Evaluation of QAM System with a Receiver Designed for Impulsive Noise

In [5], [7], [8], we have investigated the maximum likelihood detection methods for class A impulsive noise. In this section, we give the construction of the receiver which performs maximum likelihood detection under class A impulsive noise environment, and evaluate the performance of QAM systems with this receiver.

A. Construction of the Receiver Designed for Class A Impulsive Noise

Using the receiver model illustrated in Fig. 8, let us discuss the receiver designed for class A impulsive noise. If N samples are taken in one symbol duration, the received symbol $\boldsymbol{R}$ can be represented as

$$\boldsymbol{R} = \{r_1, r_2, \cdots, r_N\}, \tag{26}$$

where $r_n (1 \leq qn \leq qN)$ is the nth sample of the received symbol $\boldsymbol{R}$. In the following analysis, we assume that these N samples $r_1, r_2, \cdots, r_N$ are statistically independent. This assumption implies that the noise bandwidth at the receiver's ARI stages is N times as broad as the signal bandwidth. Let

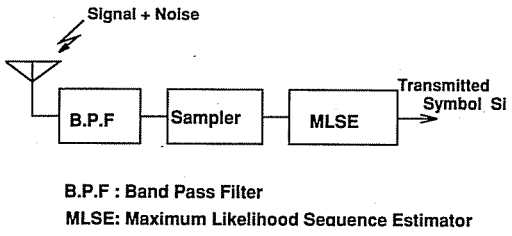

Fig. 8. Maximum likelihood detection receiver model.

r_{nx} and r_{ny} be the in-phase and quadrature components of r_n, respectively, then r_n is represented with complex value (equivalent baseband expression) as

$$r_n = r_{nx} + j r_{ny}. \tag{27}$$

Similarly, the transmitted symbol $\widehat{\boldsymbol{Si}}$ and the received noise symbol $\boldsymbol{N}$ are described as

$$\widehat{\boldsymbol{Si}} = \{\widehat{si}_1, \widehat{si}_2, \cdots, \widehat{si}_N\}, \tag{28}$$

$$\widehat{si}_n = \widehat{si}_{nx} + j\widehat{si}_{ny}, \tag{29}$$

$$\boldsymbol{N} = \{n_1, n_2, \cdots, n_N\}, \tag{30}$$

$$n_n = n_{nx} + j n_{ny}, \tag{31}$$

where

$\widehat{si}_n$ the nth sample of $\widehat{Si}$,

$\widehat{si}_{nx}, \widehat{si}_{ny}$ the in-phase component and the quadrature component of $\widehat{si}_n$,

n_n the nth sample of $\boldsymbol{N}$,

n_{nx}, n_{ny} the in-phase component and the quadrature component of n_n.

The probability that $\boldsymbol{R}$ is received, given that $\widehat{\boldsymbol{Si}}$ was sent, is expressed as

$$\begin{aligned} \mathrm{Prob}(\boldsymbol{R}|\widehat{\boldsymbol{Si}}) &= \mathrm{Prob}(\boldsymbol{N} = \boldsymbol{R} - \widehat{\boldsymbol{Si}}) \\ &= \prod_{n=1}^{N} p(r_n - \widehat{si}_n). \end{aligned} \tag{32}$$

In general, the probability given in (32) is called "likelihood." A receiver based on the maximum likelihood detection selects the symbol that maximizes this equation for given $\boldsymbol{R}$. The receiver with this strategy minimizes the symbol error probability, and in this sense, a receiver which performs maximum likelihood detection is called to be an optimum receiver.

Substituting the joint pdf of the in-phase and quadrature components (11) into (32), we can obtain the likelihood for class A impulsive noise as

$$\begin{aligned} &\mathrm{Prob}(\boldsymbol{R}|\widehat{\boldsymbol{Si}}) \\ &= \prod_{n=1}^{N} \left[e^{-A} \sum_{m=0}^{\infty} \frac{A^m}{m! \pi \sigma_m^2} \right. \\ &\quad \left. \cdot \exp\left\{ -\frac{(r_{nx} - \widehat{si}_{nx})^2 + (r_{ny} - \widehat{si}_{ny})^2}{\sigma_m^2} \right\} \right]. \end{aligned} \tag{33}$$

The receiver, which performs maximum likelihood detection under class A impulsive noise environment, selects the symbol $\widehat{Si}$ that maximizes (33) as transmitted one. Designing

the receiver based on this complicated equation has a great difficulty.

Under the condition that the impulsive index A is sufficiently small, the infinite sum in (2) can be approximated by the maximum value of its first three terms [5]. According to this approximation, the joint pdf of the in-phase and quadrature components (11) becomes

$$\tilde{p}_{x,y}(x,y) = \max_{m=0,1,2}\left[e^{-A}\frac{A^m}{m!2\pi\sigma_m^2}\exp\left\{-\frac{x^2+y^2}{2\sigma_m^2}\right\}\right], \tag{34}$$

that is,

$$\tilde{p}_{x,y}(x,y) = \begin{cases} e^{-A}\dfrac{1}{2\pi\sigma_0^2}\exp\left\{-\dfrac{x^2+y^2}{2\sigma_0^2}\right\} \\ \quad \triangleq \tilde{p}_0 \quad (0 \le |x^2+y^2| < a) \\ e^{-A}\dfrac{A}{2\pi\sigma_1^2}\exp\left\{-\dfrac{x^2+y^2}{2\sigma_1^2}\right\} \\ \quad \triangleq \tilde{p}_1 \quad (a \le |x^2+y^2| < b) \\ e^{-A}\dfrac{A^2}{4\pi\sigma_2^2}\exp\left\{-\dfrac{x^2+y^2}{2\sigma_2^2}\right\} \\ \quad \triangleq \tilde{p}_2 \quad (b \le |x^2+y^2|), \end{cases} \tag{35}$$

where a and b are given from $\tilde{p}_0(a) = \tilde{p}_1(a)$ and $\tilde{p}_1(b) = \tilde{p}_2(b)$ as

$$a = \frac{2\sigma_0^2\sigma_1^2}{\sigma_0^2-\sigma_1^2}\ln\left(\frac{\sigma_0^2}{\sigma_1^2}A\right),$$
$$b = \frac{2\sigma_1^2\sigma_2^2}{\sigma_1^2-\sigma_2^2}\ln\left(\frac{\sigma_1^2}{2\sigma_2^2}A\right). \tag{36}$$

Using this approximated joint pdf, we can see that finding the transmitted symbol that maximizes (33) is equivalent to the selection of the symbol that maximizes the following equation

$$\tilde{\Lambda}(\widehat{Si}) = \sum_{n=1}^{N}\left\{\max_{m=0,1,2}\left[-\frac{(r_{nx}-\widehat{si}_x)^2+(r_{ny}-\widehat{si}_y)^2}{\sigma_m^2} + \ln\frac{A^m}{m!\sigma_m^2}\right]\right\}$$
$$= -\sum_{n=1}^{N}\left\{\min_{m=0,1,2}\left[\frac{(r_{nx}-\widehat{si}_x)^2+(r_{ny}-\widehat{si}_y)^2}{\sigma_m^2} - \ln\frac{A^m}{m!\sigma_m^2}\right]\right\}.$$
$$(\text{for } M-\text{ary signal} \qquad i = 0,1,\cdots,M-1)., \tag{37}$$

As the result, from (37), the optimum receiver, which performs maximum likelihood detection of a 16-ary signal under class A impulsive noise environment by finding the symbol that maximizes $\tilde{\Lambda}(\widehat{Si})$, is obtained as shown in Fig. 9.

B. Simulation Results

To show the performance of the optimum receiver given above, we have made numeric simulation. The results are shown in Fig. 10. From this figure, we can find that the performance of QAM systems with the optimum receiver designed for impulsive noise is much better than that with the conventional receiver and the great performance improvement is achieved by the receiver designed for impulsive noise. In the case of impulsive index $A = 0.1$, for example, the performance improvement is about 40 dB at symbol error probability $= 10^{-2}$. It is also observed from Fig. 10 that the greater performance improvement at low symbol error probability is obtained with the smaller impulsive index A (i.e., higher impulsiveness).

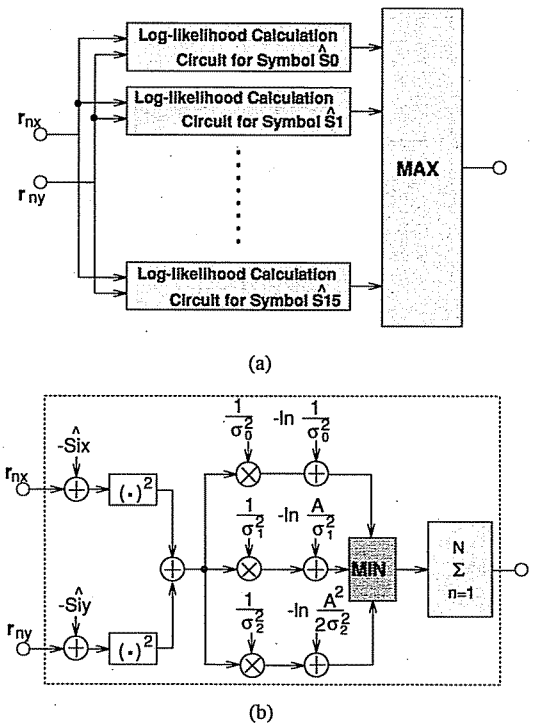

Fig. 9. Construction of the Maximum Likelihood (ML) receiver for 16 QAM signal under class A impulsive noise environment.

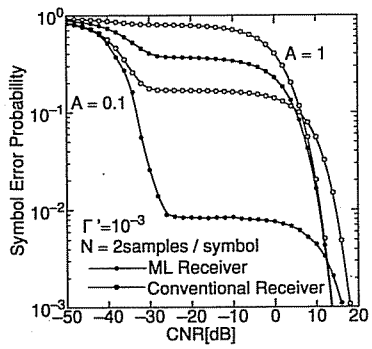

Fig. 10. Symbol error probabilities of QAM systems with the conventional receiver and the ML receiver.

V. Conclusion

We have investigated the performance of QAM systems under class A impulsive noise environment. First, we have discussed the dependence between the in-phase and quadrature components of the noise, and shown that these components can be assumed to be independent only with the large impulsive index. Next, with consideration of the dependence of the in-

phase and quadrature components of the impulsive noise, we have derived the symbol error probability of QAM systems with the conventional receiver. Numerical results conclude that a coarse assumption where the in-phase and quadrature components are independent gives an upper bound of the symbol error rate performance. We have also considered the receiver which performs maximum likelihood detection under class A impulsive noise environment, and shown the great performance improvement achieved by this receiver.

REFERENCES

[1] J. C. Y. Huang, K. Kohiyama, A. Leclert, and F. Siebelink, "Advances in digital radio communication by radio: Guest editorial," *IEEE J. Select. Areas Commun.*, vol. SAC-5, pp. 317–320, Apr. 1987.

[2] S. Sampei, "Rayleigh fading compensation method for 16 QAM modem in digital land mobile radio systems," (in Japanese) *Trans. IEICE Jap.*, vol. J72-BII, pp. 7–15, Jan. 1989.

[3] D. Middleton, "Statistical-physical models of electromagnetic interference," *IEEE Trans. Electromagn. Compat.*, vol. EMC-19, pp. 106–126, Aug. 1977.

[4] A. D. Spaulding and D. Middleton, "Optimum reception in an impulsive interference environment—Part I: Coherent detection," *IEEE Trans. Commun.*, vol. COM-25, pp. 910–923, Sept. 1977.

[5] H. Kusao, N. Morinaga, and T. Namekawa, "Optimum coherent receiver for impulsive RF noise," (in Japanese) *Trans. IECE Jap.*, vol. J68-B, pp. 684–691, June 1985.

[6] J. S. Seo, S. J. Cho, and K. Feher, "Impact of non-Gaussian noise on the performance of high-level QAM," *IEEE Trans. Electromagn. Compat.*, vol. EMC-31, pp. 177–180, May 1989.

[7] S. Miyamoto, M. Katayama, and N. Morinaga, "Signal detection characteristics in trellis coded modulation system under impulsive noise environment and its optimum reception," (in Japanese) *Trans. IEICE Jap.*, vol. J68-BII, pp. 671–681, Oct. 1992.

[8] S. Miyamoto, M. Katayama, and N. Morinaga, "Optimum detection and design of TCM signals under impulsive noise environment," in *Proc. IEEE Int. Conf. Syst. Eng.*, Sept. 1992, pp. 473–478.

[9] L. A. Berry, "Understanding middleton's canonical formula for class A noise," *IEEE Trans. Electromagn. Compat.*, vol. EMC-23, pp. 337–344, Nov. 1981.

[10] D. Middleton, "Canonical and quasi-canonical probability models of class A interference," *IEEE Trans. Electromagn. Compat.*, vol. EMC-25, pp. 76–106, May 1983.

[11] ———, "Canonical non-Gaussian noise models: Their implication for measurement and for prediction of receiver performance," *IEEE Trans. Electromagn. Compat.*, vol. EMC-21, pp. 209–220, Aug. 1979.

Shinichi Miyamoto (M'94) was born in Kobe, Japan, on April 16, 1966. He received the B.E. and M.E. degrees in communication engineering from Osaka University, Japan in 1990 and 1992, respectively.

He is currently a Research Assistant in the Department of Communication Engineering at Osaka University. His current research interests include digital radio communications systems under man-made noise environment.

Mr. Miyamoto is a member of IEICE of Japan.

Masaaki Katayama (S'82–M'86) was born in Kyoto, Japan in 1959. He received the B.S., M.S., and Ph.D. degrees from Osaka University, Japan in 1981, 1983, and 1986, respectively, all in communication engineering.

In 1986, he was an Assistant Professor at Toyohashi University of Technology, Japan, and had been a Lecturer at Osaka University from 1989 to 1992. Since 1992, he has been an Associate Professor of the Department of Information Electronics at Nagoya University, Japan. His current research interests include satellite and mobile communication systems, spread-spectrum modulation schemes, nonlinear digital modulations and coded modulations, communications under non-Gaussian noise and fading environment and computer networks.

Dr. Katayama received the IECE Shinohara Memorial Young Engineer Award in 1986. He is a member of IEICE of Japan, SITA, and the Information Processing Society of Japan.

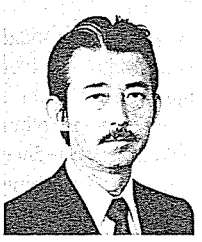

Norihiko Morinaga (S'64–M'68–SM'92) was received the B.E. degree in electrical engineering from Shizuoka University, Shizuoka, Japan, in 1963, and the M.E. and the Ph.D. degree from Osaka University, Osaka, Japan, in 1965 and 1968, respectively.

He is currently a Professor in the Department of Communication Engineering at Osaka University, working in the area of radio, mobile, satellite and optical communication systems, and system EMC.

Dr. Morinaga is a member of the IEICE and the Institute of Television Engineering of Japan.